Progress In Electromagnetics Research M, Vol. 94, 61–71, 2020

Design of Dual-Beam Reflection Based on 2-Bit Coding Metasurfaces

Honggang Hao, Ting Zhang*, Wei Ruan, and Bin Wang

Abstract—In general, a single beam reflection can be realized by 2-bit coding metasurfaces. In order to obtain multi-beam reflection, a design method for coding sequence based on 2-bit coding metasurfaces is proposed, which can manipulate the direction of reflected beams by 2-bit addition rule and control the number of reflected beams by addition theorem on complex codes. This method simplifies the design process of coding sequence, and the direction and number of multi-beams can be flexibly designed. In this paper, the design of dual-beam reflection is taken as an example to illustrate the design process of coding sequence. Both simulation and measurement results show that the designed metasurface realizes the dual-beam reflection, and the direction of reflected beams is consistent with expectations. The proposed method is of great significance for the design of multi-beam reflection based on coding metasurfaces.

1. INTRODUCTION

Metasurfaces are artificial planar structures, which are composed of periodic or non-periodic subwavelength resonators [1]. Owning to their unique electromagnetic properties, metasurfaces can effectively manipulate EM waves to realize many special functionalities, such as anomalous reflection [2, 3], polarization conversion [4, 5], and perfect absorption [6, 7]. Meanwhile, metasurfaces can also be used as spatial filters and for electric phase correction of an electromagnetic source [8, 9]. In relation to beamforming and beamsteering, all-dielectric metasurface with incremental phase shift and metasurface using printed surfaces were proposed for 2D beam steering [10, 11]. Recently nature-based optimization approaches, such as ant colony, have been extensively used for designing various types of metasurfaces [12, 13].

Lately, the concept of coding metasurfaces has been reported as a powerful wave manipulation tool [14]. In 1-bit coding metasurfaces, binary 1-bit digital codes "0" and "1" are used to represent two metasurface elements with reflection phases "0" and "π". By coding "0" and "1" with different coding sequences, EM waves can be manipulated to realize diverse functions [15–22]. The digital codes can be extended to 2-bit to generate a single beam with discrete reflection angle. The digital states "0", "1", "2", and "3" indicate the reflection phases of "0", "$\pi/2$", "π", and "$3\pi/2$", respectively. Compared with 1-bit coding metasurface, 2-bit coding metasurface has more units, so the control of electromagnetic waves is more flexible and diverse.

Based on these concepts, many researches pay more attention to the reduction of radar cross section and anomalous reflection. Recently, convolution operations on coding metasurfaces were put forward to improve the control ability and realize arbitrary radiation angle in the upper space using 2-bit coding metasurfaces [23]. Furthermore, a matrix-form-coding metasurface was proposed to flexibly control the main lobes number and azimuth angle of terahertz-transmitted beams [24]. Meanwhile, addition theorem on complex codes was presented, when two different coding sequences with different functions

Received 23 March 2020, Accepted 15 June 2020, Scheduled 8 July 2020
* Corresponding author: Ting Zhang (525986187@qq.com).
The authors are with the College of Optoelectronic Engineering, Chongqing University of Posts and Telecommunications, Chongqing, China.

were added together via this addition theorem, and the combined coding sequence could directly generate the two functions simultaneously without generating any new functions [25]. However, it is well known that the direction and number of reflected beams are difficultly controlled at the same time by simple coding sequence.

In order to achieve multi-beam reflection based on a coding metasurface, a design method for coding sequence is proposed in this paper. The direction of reflected beams can be controlled by 2-bit addition rule, and the number of reflected beams can be manipulated by addition theorem on complex codes. Using this coding method, a metasurface with dual beams is designed to reflect the normally incident EM waves to predesigned directions. Simulated and measured results demonstrate its excellent performance for dual-beam generation, and the correctness of this method is verified.

2. THEORETICAL ANALYSIS

As mentioned above, the direction and number of reflected beams can be manipulated by 2-bit addition rule and addition theorem on complex codes. Here, the theory of 2-bit addition rule and addition theorem on complex codes are introduced.

2.1. The Theory of 2-Bit Addition Rule

The principle of coding metasurface to manipulate EM waves can be analyzed by the theory of traditional phase array antennas. The coding metasurface consists of $N \times N$ lattices with the same size P in which each lattice is occupied by a sub-array of "0" or "1" elements, as shown in Fig. 1. The scattering phase of the (m, n)th lattice is assumed to be $\varphi_{(m,n)}$. Under the normal incidence of plane waves, the far-field scattering of the metasurface $f(\theta, \varphi)$ can be expressed as [14]:

$$f(\theta,\varphi) = f_e(\theta,\varphi)\sum_{m=1}^{N}\sum_{n=1}^{N}\exp\left\{-i\left\{\varphi_{(m,n)} + kP\sin\theta[(m-1/2)\cos\varphi + (n-1/2)\sin\varphi]\right\}\right\} \quad (1)$$

where θ and φ are the elevation and azimuth angles of an arbitrary direction, respectively; k is the propagation constant; and $f_e(\theta, \varphi)$ is the pattern function of a lattice. Through analysis, formula (1) can be rewritten as [26]:

$$\begin{aligned} f(\theta,\varphi) \;=\; & f_e(\theta,\varphi)\sum_{m=1}^{N}\exp\left\{-i\left[\varphi_m + kP(m-1/2)\sin\theta\cos\varphi\right]\right\} \\ & \sum_{n=1}^{N}\exp\left\{-i\left[\varphi_n + kP(n-1/2)\sin\theta\sin\varphi\right]\right\} \end{aligned} \quad (2)$$

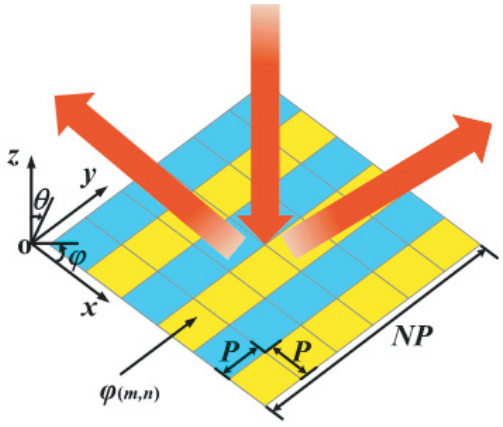

Figure 1. Schematic diagram of the principle of coding metasurface.

Table 1. 2-bit addition rule.

y direction	x direction			
	0	1	2	3
0	0	1	2	3
1	1	2	3	0
2	2	3	0	1
3	3	0	1	2

where φ_m is the scattering phase of the m-th coding element in the x-direction, and φ_n is the scattering phase of the n-th coding element in the y-direction. It can be seen from Equations (1) and (2):

$$\varphi_{(m,n)} = \varphi_m + \varphi_n \tag{3}$$

So if two coding sequences in orthogonal directions are known, a new coding sequence can be easily obtained by using Equation (3). Here, the phase responses of "0", "1", "2" and "3" are assumed as "0", "$\pi/2$", "π", and "$3\pi/2$", respectively. According to Equation (3), a 2-bit addition rule represented by "0", "1", "2", and "3" is shown in Table 1. When a new coding metasurface generated by the 2-bit addition rule is illuminated by plane waves, the reflection beam's elevation of θ and azimuthal of φ can be calculated as [26]:

$$\varphi = \pm \tan^{-1} \frac{\Gamma_x}{\Gamma_y}, \quad \varphi = \pi \pm \tan^{-1} \frac{\Gamma_x}{\Gamma_y} \tag{4}$$

$$\theta = \sin^{-1} \left(\lambda \cdot \sqrt{\frac{1}{\Gamma_x^2} + \frac{1}{\Gamma_y^2}} \right) \tag{5}$$

where λ is the free-space wavelength at the working frequency, and Γ_x and Γ_y are the physical periodic lengths of the phase gradient coding sequence along x and y directions, respectively. If the reflection angle of a single-beam is known, then Γ_x and Γ_y can be calculated by Equations(4) and (5). And the 2-bit coding sequences along x and y directions can be designed according to Γ_x and Γ_y. With the application of the 2-bit addition rule, a single beam with pre-designed direction can be easily and conveniently realized.

2.2. The Theory of Addition Theorem on Complex Codes

In general, the coding metasurface only uses the absolute phase value φ for coding. In order to retain all the information of phase, the complex digital codes and an addition theorem on complex codes were proposed by Ruiyuan Wu and others. The complex digital codes used the whole phase term $e^{j\varphi}$ to define the digital states. The addition operation of two complex codes was: $e^{j\varphi_1} + e^{j\varphi_2} = e^{j\varphi}$, in which φ_1 and φ_2 were the arguments of the two complex digital codes. After addition, a complex number with argument φ was got. The addition operation results could be obtained by the vector superposition principle in the traditional Euclidean geometry. The final regulations for addition operations on 2-bit complex digital codes are shown in Table 2 [25]. (The top dot indicates the complex property, and the number at the bottom right corner represents the bit of digital state).

Table 2. Addition theorem on 2-bit complex digital codes.

$\dot{0}_2 + \dot{0}_2 = \dot{0}_3$	$\dot{1}_2 + \dot{0}_2 = \dot{1}_3$	$\dot{2}_2 + \dot{0}_2 = \dot{6}_3$	$\dot{3}_2 + \dot{0}_2 = \dot{7}_3$
$\dot{0}_2 + \dot{1}_2 = \dot{1}_3$	$\dot{1}_2 + \dot{1}_2 = \dot{2}_3$	$\dot{2}_2 + \dot{1}_2 = \dot{3}_3$	$\dot{3}_2 + \dot{1}_2 = \dot{0}_3$
$\dot{0}_2 + \dot{2}_2 = \dot{2}_3$	$\dot{1}_2 + \dot{2}_2 = \dot{3}_3$	$\dot{2}_2 + \dot{2}_2 = \dot{4}_3$	$\dot{3}_2 + \dot{2}_2 = \dot{5}_3$
$\dot{0}_2 + \dot{3}_2 = \dot{7}_3$	$\dot{1}_2 + \dot{3}_2 = \dot{4}_3$	$\dot{2}_2 + \dot{3}_2 = \dot{5}_3$	$\dot{3}_2 + \dot{3}_2 = \dot{6}_3$

When two different coding patterns with different functions are added via the addition theorem in complex form, the combined coding pattern will generate two functions simultaneously without any perturbations. For example, two coding sequences of 01230123... along the x-direction and 01230123... along the y-direction are added to get a new coding sequence, which can radiate two beams to the directions of $\varphi = 0°$ and $\varphi = 90°$. The combination of 2-bit addition rule and addition theorem on complex codes forms a new coding sequence, so as to realize multi-beam reflection with predesigned directions.

3. DESIGN OF CODING METASURFACE

In order to design a coding metasurface which can simultaneously generate dual beams with the directions of $\varphi = 90°$ and $\varphi = 315°$, metasurface elements are designed first. Then, arranging the metasurface elements according to the designed coding sequence achieves the dual-beam reflection metasurface.

3.1. The Element Design of Coding Metasurface

The element structure is composed of three layers as shown in Fig. 2. An F4B dielectric substrate is chosen as the middle layer with thickness $h = 1.5\,\text{mm}$, dielectric constant $\varepsilon_r = 2.65$, and loss tangent $\tan\delta = 0.001$. The surface of the dielectric substrate is fabricated with copper with a thickness $h_1 = 0.018\,\text{mm}$, and the structure is shown in Fig. 2(a), on the bottom of the dielectric substrate is a metal backboard.

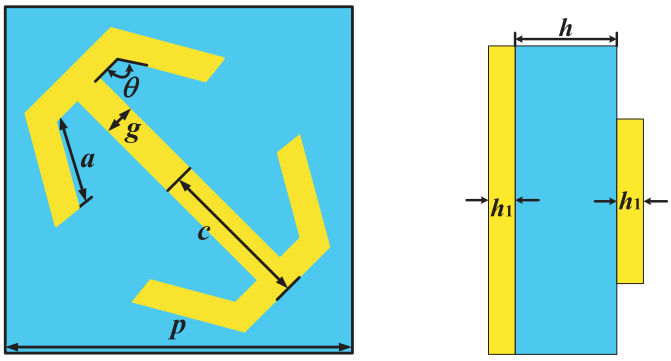

Figure 2. Schematic of the coding metasurface element. (a) The top view. (b) The side view.

Parameter a has a great effect in the design of the structure. Considering the application scenarios of 5G millimeter wave, the optimized geometrical parameter a for the 1-bit, 2-bit, and 3-bit coding elements is shown in Table 3. Other structural parameters of the element are: $p = 3.5\,\text{mm}$, $g = 0.3\,\text{mm}$, $c = 1.5\,\text{mm}$, and $\theta = 120°$.

The simulated results of the reflection amplitude and phase are all obtained by using CST Microwave Studio, as shown in Fig. 3. In the simulation process, the boundary conditions along the x and y directions are "unit cell". At operation frequency of 28 GHz, it can be seen that the reflection phases of the eight coding elements are $-176°$, $-223°$, $-270°$, $-320°$, $-356°$, $-403°$, $-450°$, and $-500°$, respectively, and their reflection amplitudes are close to 1.'

3.2. The Design of Coding Metasurface

Based on the 2-bit addition rule and addition theorem on complex codes, a coding metasurface with multi-beam reflection can be realized. Considering the limitation of measured conditions, a coding metasurface with dual-beam reflection of $\varphi = 90°$ and $\varphi = 315°$ is designed as an example. In the design process, the single beam is generated by the 2-bit addition rule, and the beam's elevation and

Table 3. The schematic diagrams of the eight elements.

No.	0	1	2	3	4	5	6	7
Unit cells	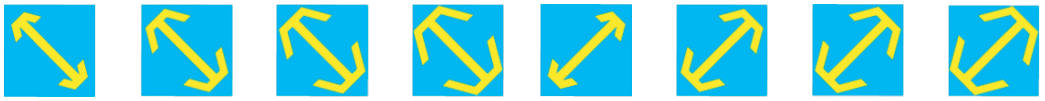							
a (mm)	0.3	0.6	0.8	1.0	0.3	0.6	0.8	1.0
1-bit	01	×	×	×	11	×	×	×
2-bit	02	×	12	×	22	×	32	×
3-bit	03	13	23	33	43	53	63	73

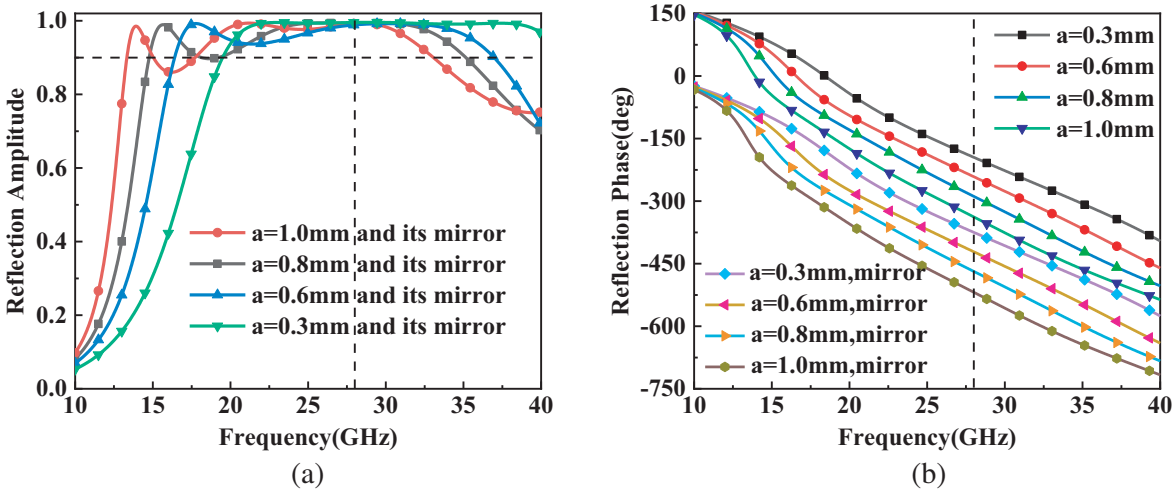

Figure 3. Reflection characteristic of the elements. (a) Reflection amplitude. (b) Reflection phase.

azimuth angles can be calculated according to Equations (4) and (5). Then, the two coding sequences of $\varphi = 90°$ and $\varphi = 315°$ are added to get a new coding sequence with dual-beam reflection by the addition theorem on complex codes. The designed metasurface consists of 20×20 coding lattices, and each coding lattice is composed of a 2×2 array of equal phase elements. The specific design process is as follows.

Firstly, a reflection beam with $\varphi = 315°$ is generated by the 2-bit addition rule, which is named B1. Since $\varphi = 315°$, Γ_x is equal to Γ_y according to Equation (4). So the coding sequences along x and y directions could be designed as S1 (0123 0123 0123 0123 0123) and S2 (3210 3210 3210 3210 3210), respectively. According to Equations (4) and (5), when the coding sequence is S1, the normally incident EM waves will be reflected into the directions of $\varphi = 0°$ and $\theta = 22.5°$. When the coding sequence is S2, the normally incident EM waves will be reflected into the directions of $\varphi = 270°$ and $\theta = 22.5°$. Then, the two coding sequences are combined to get B1 by using 2-bit addition rule. When the coding sequence is B1, the normally incident EM waves will be reflected into the directions of $\varphi = 315°$ and $\theta = 32.8°$. The coding patterns and theoretical far-field scattering patterns calculated by Matlab at 28 GHz are shown in Fig. 4.

Then, a reflection beam named B2 is designed which could be the coding sequence (0123 0123 0123 0123 0123) along y-direction. According to Equations (4) and (5), the normally incident EM waves will be reflected into the directions of $\varphi = 90°$ and $\theta = 22.5°$ at 28 GHz. The coding patterns and theoretical far-field scattering patterns calculated by Matlab at 28 GHz are shown in Fig. 5(a) and Fig. 5(c).

Finally, B1 and B2 are added together via the addition theorem on complex codes to get a new coding pattern which is named B, and B has the characteristics of B1 and B2 at the same time. The

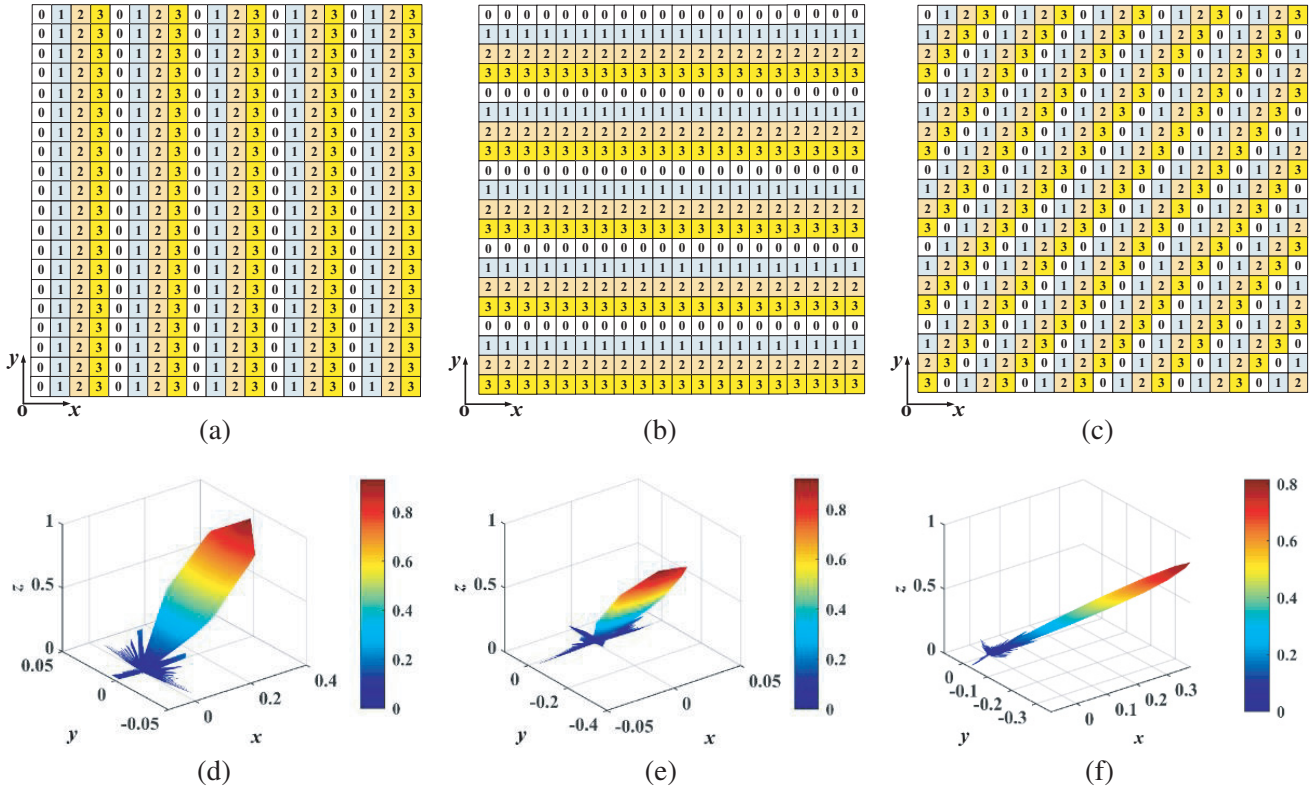

Figure 4. Coding patterns and their 3D theoretical scattering patterns calculated by Matlab. (a) The coding patterns of S1. (b) The coding patterns of S2. (c) The coding patterns of B1. (d) The 3D far-field scattering patterns of S1. (e) The 3D far-field scattering patterns of S2. (f) The 3D far-field scattering patterns of B1.

coding patterns and theoretical far-field scattering patterns calculated by Matlab at 28 GHz are shown in Fig. 5(b) and Fig. 5(d).

In order to verify this theoretical design, the CST Microwave Studio is used to model and simulate the coding metasurface. An x-polarized plane wave is normally incident into the coding metasurface with "open (add space)" boundary condition. The simulated far-field scattering patterns with different coding sequences are shown in Fig. 6. When the coding sequence is B1, the normally incident EM waves will be reflected into the directions of $\varphi = 315°$ and $\theta = 33.3°$. When the coding sequence is B2, the normally incident EM waves will be reflected into the directions of $\varphi = 90°$ and $\theta = 22.6°$. When the coding sequence is B, the normally incident EM waves will be reflected into two beams, one of which is at the directions of $\varphi = 315°$ and $\theta = 33.3°$ and the other at the direction of $\varphi = 90°$ and $\theta = 22.6°$, which have very good agreements with the theoretical calculation. Notice that the designed metasurface unit structure is a polarization conversion unit, so the polarization of reflected wave is along the y direction.

4. MEASUREMENT AND DISCUSSION

In order to verify the design, a coding metasurface sample is fabricated using the printed circuit board technology, and the sample contains 40×40 elements with a size of 140 mm $\times$ 140 mm as shown in Fig. 7(a).

The far-field measurement is performed in a standard microwave anechoic chamber, and the environment is shown in Fig. 7(b). The positions of the feeding antenna, receiving antenna, and sample are at the same height. A horn antenna with working bandwidth from 10 to 40 GHz is employed as the feeding antenna to generate the plane wave for the coding metasurface. Both the feeding antenna and sample are coaxially mounted on a board which can automatically rotate 360° with 1° step in the

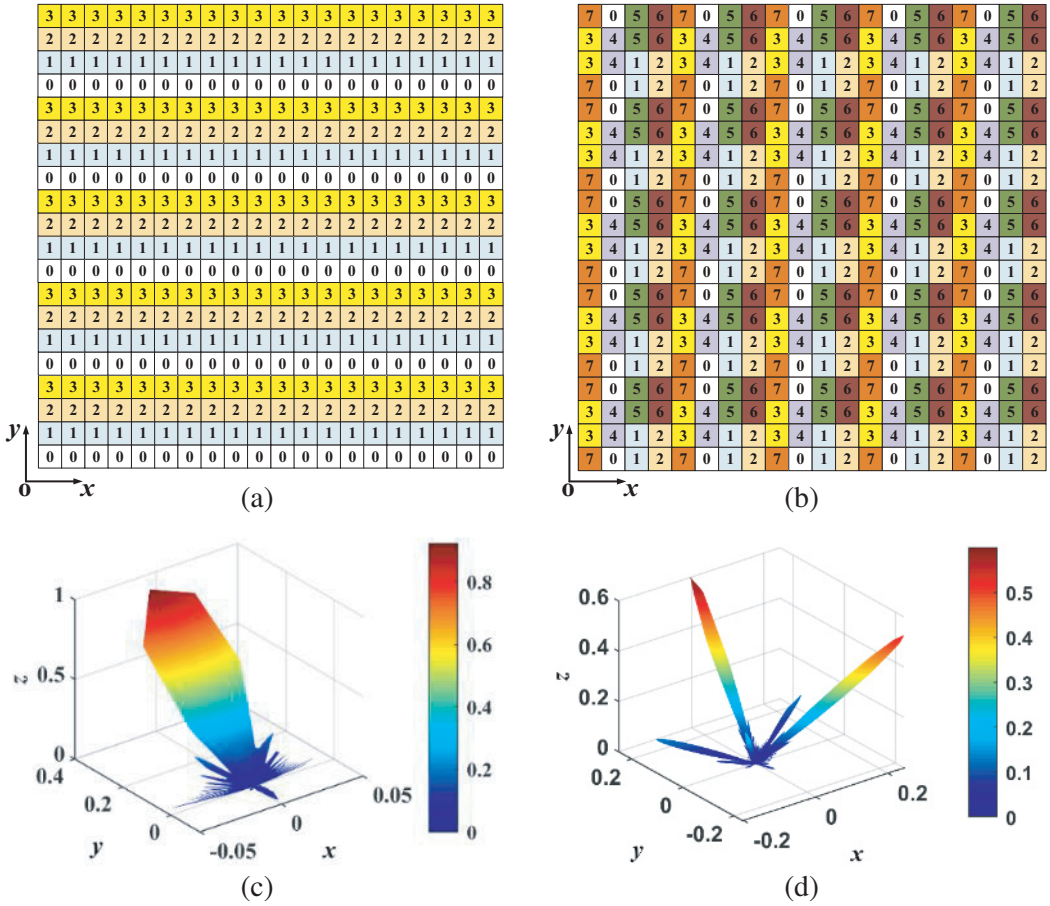

Figure 5. Coding patterns and their 3D theoretical scattering patterns calculated by Matlab. (a) The coding patterns of B2. (b) The coding patterns of B. (c) The 3D far-field scattering patterns of B2. (d) The 3D far-field scattering patterns of B.

horizontal plane. The receiving antenna automatically records the electric fields in the horizontal plane.

The simulated and measured results of 2D scattering pattern are shown in Fig. 8. The scattering pattern of coding metasurface in *yoz* plane is shown in Fig. 8(a), and the center of the measurement scattering peak appears at the angle of $\theta = 28°$. The scattering pattern of coding metasurface in $\varphi = 315°/135°$ plane is shown in Fig. 8(b), and the center of the measurement scattering peak appears at the angle of $\theta = 29°$. It can be seen in Table 4 that the deviations between simulation and measurement are about 5°, and the differences are mainly attributed to the misalignment of the feeding antenna, sample, and receiving antenna during the experiment. The disagreement in the shapes of the main beam and side lobes is mainly due to the sample which is not in the center of rotation. Overall, the proposed metasurface performs well.

Table 4. Comparison of simulated and measured results.

	$\varphi = 90°$ plane	$\varphi = 315°$ plane
Simulated results	$\theta = 22.6°$	$\theta = 33.3°$
Measured results	$\theta = 28°$	$\theta = 29°$

This paper designs dual-beam reflection as an example, and any two arbitrary beams can be synthesized by using this approach. The design method of multi-beam reflection is similar to the dual-

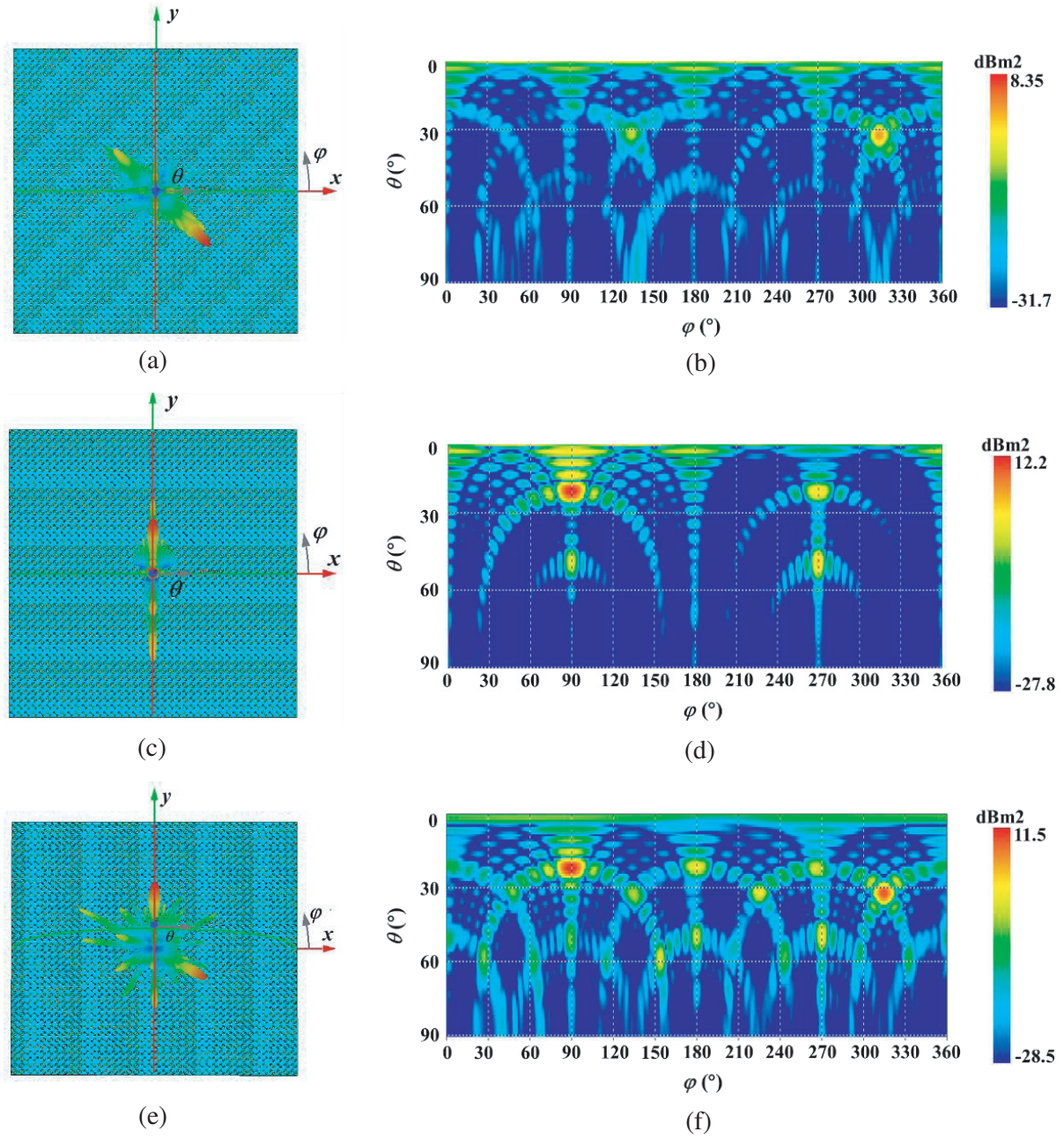

Figure 6. Simulated far-field scattering by CST at 28 GHz. (a) The 3D scattering patterns of B1. (b) The 2D scattering patterns of B1. (c) The 3D scattering patterns of B2. (d) The 2D scattering patterns of B2. (e) The 3D scattering patterns of B. (f) The 2D scattering patterns of B.

beam design. Here, a design idea is provided, and the design of three-beam reflection is taken as an example. Firstly, using the 2-bit addition rule designs three sets of coding sequences with predesigned reflection angles, and the three sets of coding sequence are named B1, B2, and B3, respectively. Then, B1 and B2 are added together according to the addition theorem on complex codes to get the new coding sequence which is named as B4. Finally, B3 and B4 are added together via the addition theorem on complex codes to get the coding sequence which can simultaneously generate predesigned three-beams. Note that the addition theorem on complex codes needs to be extended to more bits.

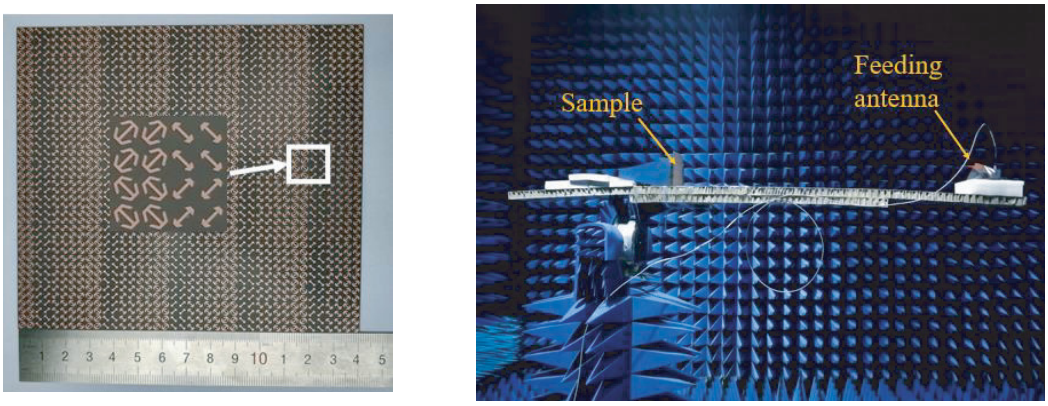

(a) (b)

Figure 7. The fabricated sample and experimental setup. (a) The fabricated sample. (b) The experimental setup.

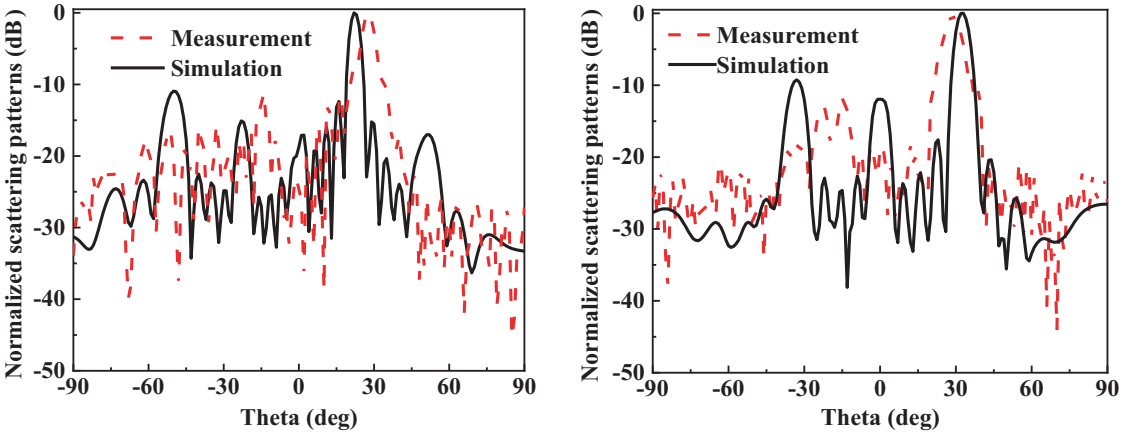

(a) (b)

Figure 8. The simulation and measurement results at 28 GHz. (a) The *yoz* plane. (b) The $\varphi = 315°/135°$ plane.

5. CONCLUSION

Based on the 2-bit addition rule and the addition theorem on complex codes, this paper presents a design method for generating multi-beams with predesigned directions at the same time. Then, the design of dual-beam reflection with azimuths of 90° and 315° is taken as an example to show the design process. The metasurface is designed by adopting a hexagonal arrow structure as the metasurface element. The consistency of the simulated and measured results indicates the powerful potentials of the proposed coding metasurface in controlling the EM waves. The proposed design method is meaningful for multi-beam reflection based on coding metasurface.

ACKNOWLEDGMENT

This work was supported by the Natural Science Foundation of Chongqing, China (No. cstc2018jcyjAX0508) and by the Science and Technology Research Program of Chongqing Municipal Education Commission (Grant No. KJQN201800639).

REFERENCES

1. Holloway, C. L., E. F. Kuester, J. A. Gordon, et al., "An overview of the theory and applications of metasurfaces: The two-dimensional equivalents of metamaterials," *IEEE Antennas and Propagation Magazine*, Vol. 54, No. 2, 10–35, 2012.
2. Yu, N., P. Genevet, M. A. Kats, et al., "Light propagation with phase discontinuities: Generalized laws of reflection and refraction," *Science*, Vol. 334, No. 6054, 333–337, 2011.
3. Li, Z. W., L. R. Huang, K. Lu, et al., "Continuous metasurface for high-performance anomalous reflection," *Applied Physics Express*, Vol. 7, No. 11, 112001, 2014.
4. Sun, H., C. Gu, X. Chen, et al., "Ultra-wideband and broad-angle linear polarization conversion metasurface," *Journal of Applied Physics*, Vol. 121, No. 17, 174902, 2017.
5. Zang, X. F., H. H. Gong, Z. Li, et al., "Metasurface for multi-channel terahertz beam splitters and polarization rotators," *Applied Physics Letters*, Vol. 112, No. 17, 171111, 2018.
6. Savo, S., D. Shrekenhamer, and W. J. Padilla, "Liquid crystal metamaterial absorber spatial light modulator for THz applications," *Advanced Optical Materials*, Vol. 2, No. 3, 275–279, 2014.
7. Liu, S., H. Chen, and T. J. Cui, "A broadband terahertz absorber using multi-layer stacked bars," *Applied Physics Letters*, Vol. 106, No. 15, 151601, 2015.
8. Lalbakhsh, A., M. U. Afzal, K. P. Esselle, et al., "Multi-objective particle swarm optimization for the realization of a low profile bandpass frequency selective surface," *International Symposium on Antennas and Propagation*, 809–812, 2015.
9. Lalbakhsh, A., M. U. Afzal, and K. P. Esselle, "Simulation-driven particle swarm optimization of spatial phase shifters," *International Conference on Electromagnetics in Advanced Applications*, 428–430, 2016.
10. Afzal, M. U., A. Lalbakhsh, and K, P. Esselle, "Electromagnetic-wave beam-scanning antenna using near-field rotatable graded-dielectric plates," *Journal of Applied Physics*, Vol. 124, No. 23, 234901, 2018.
11. Afzal, M. U., K. P. Esselle, and A. Lalbakhsh, "A metasurface to focus antenna beam at offset angle," *2018 2nd URSI Atlantic Radio Science Meeting (AT-RASC)*, 1–4, 2018.
12. Zhu, D. Z., E. B. Whiting, S. D. Campbell, et al., "Optimal high efficiency 3D plasmonic metasurface elements revealed by lazy ants," *ACS Photonics*, Vol. 6, No. 11, 2741–2748, 2019.
13. Lalbakhsh, P., B. Zaeri, and A. Lalbakhsh, "An improved model of ant colony optimization using a novel pheromone update strategy," *ICE Transactions on Information and Systems*, Vol. 96, No. 11, 2309–2318, 2013.
14. Cui, T. J., M. Q. Qi, X. Wan, et al., "Coding metamaterials, digital metamaterials and programmable metamaterials," *Light: Science & Applications*, Vol. 3, No. 10, e218, 2014.
15. Hao, H., S. Du, and T. Zhang, "Small-size broadband coding metasurface for RCS reduction based on particle swarm optimization algorithm," *Progress In Electromagnetics Research M*, Vol. 81, 97–105, 2019.
16. Zhou, Y., X. Y. Cao, J. Gao, et al., "RCS reduction for grazing incidence based on coding metasurface," *Electronics Letters*, Vol. 53, No. 20, 1381–1383, 2017.
17. Liu, G., J. Liu, S. Zhao, et al., "Ultra-wideband low-detectable coding metasurface," *Chinese Journal of Electronics*, Vol. 28, No. 6, 1265–1270, 2019.
18. Jing, H. B., Q. Ma, G. D. Bai, et al., "Anomalously perfect reflections based on 3-Bit coding metasurfaces," *Advanced Optical Materials*, Vol. 7, No. 9, 1801742, 2019.
19. Gao, X., W. L. Yang, H. F. Ma, et al., "A reconfigurable broadband polarization converter based on an active metasurface," *IEEE Transactions on Antennas and Propagation*, Vol. 66, No. 11, 6086–6095, 2018.
20. Su, J., H. He, Z. Li, et al., "Uneven-layered coding metamaterial tile for ultra-wideband RCS reduction and diffuse scattering," *Scientific Reports*, Vol. 8, No. 1, 8182, 2018.
21. Sun, H., C. Gu, X. Chen, et al., "Broadband and broad-angle polarization-independent metasurface for radar cross section reduction," *Scientific Reports*, Vol. 7, 40782, 2017.

22. Bai, G. D., Q. Ma, W. K. Cao, et al., "Manipulation of electromagnetic and acoustic wave behaviors via shared digital coding metallic metasurface," *Advanced Intelligent Systems*, Vol. 1, No. 5, 1900038, 2019.
23. Liu, S., T. J. Cui, L. Zhang, et al., "Convolution operations on coding metasurface to reach flexible and continuous controls of terahertz beams," *Advanced Science*, Vol. 3, No. 10, 1600156, 2016.
24. Fang, B., X. Bie, Z. Yan, et al., "Manipulation of main lobe number and azimuth angle of terahertz-transmitted beams by matrix-form-coding metasurface," *Applied Physics A*, Vol. 125, No. 9, 651, 2019.
25. Wu, R. Y., C. B. Shi, S. Liu, et al., "Addition theorem for digital coding metamaterials," *Advanced Optical Materials*, Vol. 6, No. 5, 1701236, 2018.
26. Jing, Y., Y. Li, J. Zhang, et al., "Fast coding method of metasurfaces based on 1D coding in orthogonal directions," *Journal of Physics D: Applied Physics*, Vol. 51, No. 47, 475103, 2018.